

Hole injection and efficiency droop improvement in InGaN/GaN light-emitting diodes by band-engineered electron blocking layer

C. H. Wang, C. C. Ke, C. Y. Lee, S. P. Chang, W. T. Chang, J. C. Li, Z. Y. Li, H. C. Yang, H. C. Kuo, T. C. Lu, and S. C. Wang

Citation: *Applied Physics Letters* **97**, 261103 (2010); doi: 10.1063/1.3531753

View online: <http://dx.doi.org/10.1063/1.3531753>

View Table of Contents: <http://scitation.aip.org/content/aip/journal/apl/97/26?ver=pdfcov>

Published by the [AIP Publishing](#)

Articles you may be interested in

[Improved carrier injection and efficiency droop in InGaN/GaN light-emitting diodes with step-stage multiple-quantum-well structure and hole-blocking barriers](#)

Appl. Phys. Lett. **102**, 241108 (2013); 10.1063/1.4811735

[Improved hole distribution in InGaN/GaN light-emitting diodes with graded thickness quantum barriers](#)

Appl. Phys. Lett. **102**, 243504 (2013); 10.1063/1.4811698

[Efficiency and droop improvement in green InGaN/GaN light-emitting diodes on GaN nanorods template with SiO₂ nanomasks](#)

Appl. Phys. Lett. **101**, 233104 (2012); 10.1063/1.4768950

[Promotion of hole injection enabled by GaInN/GaN light-emitting triodes and its effect on the efficiency droop](#)

Appl. Phys. Lett. **99**, 181115 (2011); 10.1063/1.3658388

[Efficiency droop alleviation in InGaN/GaN light-emitting diodes by graded-thickness multiple quantum wells](#)

Appl. Phys. Lett. **97**, 181101 (2010); 10.1063/1.3507891

The advertisement features a dark blue background with a grid of images showing various surface topographies. The text is in white and orange. The Oxford Instruments logo is in the top right corner. The main headline is 'NEW! Asylum Research MFP-3D Infinity™ AFM' in white, with 'Unmatched Performance, Versatility and Support' in orange below it. The Oxford Instruments logo is in the top right corner, with the tagline 'The Business of Science®' below it. The advertisement highlights four key features: 'Stunning high performance' (with a blue and white topography image), 'Simpler than ever to GetStarted™' (with a brown and orange topography image), 'Comprehensive tools for nanomechanics' (with a yellow and brown topography image), and 'Widest range of accessories for materials science and bioscience' (with a yellow and brown topography image). A photograph of the MFP-3D Infinity AFM system is shown in the bottom right corner.

Hole injection and efficiency droop improvement in InGaN/GaN light-emitting diodes by band-engineered electron blocking layer

C. H. Wang,^{1,a)} C. C. Ke,¹ C. Y. Lee,¹ S. P. Chang,^{1,2} W. T. Chang,³ J. C. Li,^{1,b)}
Z. Y. Li,¹ H. C. Yang,² H. C. Kuo,^{1,c)} T. C. Lu,¹ and S. C. Wang¹

¹Department of Photonics and Institute of Electro-Optical Engineering, National Chiao-Tung University, Hsinchu 300, Taiwan

²R&D Division, Epistar Co. Ltd., Science-based Industrial Park, Hsinchu 300, Taiwan

³Department of Electro-Physics, National Chiao-Tung University, Hsinchu 300, Taiwan

(Received 5 November 2010; accepted 6 December 2010; published online 28 December 2010)

A graded-composition electron blocking layer (GEBL) with aluminum composition increasing along the [0001] direction was designed for c-plane InGaN/GaN light-emitting diodes (LEDs) by employing the band-engineering. The simulation results demonstrated that such GEBL can effectively enhance the capability of hole transportation across the EBL as well as the electron confinement. Consequently, the LED with GEBL grown by metal-organic chemical vapor deposition exhibited lower forward voltage and series resistance and much higher output power at high current density as compared to conventional LED. Meanwhile, the efficiency droop was reduced from 34% in conventional LED to only 4% from the maximum value at low injection current to 200 A/cm². © 2010 American Institute of Physics. [doi:10.1063/1.3531753]

Solid-state lighting offers much potential to save energy and enhance the quality of our building environments, especially refers to GaN-based light-emitting diodes (LEDs).¹ For high power application of solid-state lighting, LEDs have to be operated at a very high current density, while efficiency droop would be introduced.² Carrier overflow out of the active region as well as inefficient injection and transportation of holes have been identified to be the major reasons of efficiency droop.^{3,4} To reduce the carrier overflow, an Al_xGa_{1-x}N electron blocking layer (EBL) was adopted in common LED structures. However, it has been reported that the large polarization field in Al_xGa_{1-x}N EBL reduces the effective barrier height for electrons.⁵ Therefore, the carrier overflow cannot be suppressed effectively. On the other hand, the polarization-field induced band bending and the valence band offset (ΔE_v) at the interfaces of GaN and EBL are considered to retard the injection of holes.^{2,5} To reduce the polarization field in EBL, the polarization-matched EBLs (AlInN or AlInGaN) were proposed and demonstrated to be more effective in electron confinement.^{6,7} However, it has difficulties of realization in epitaxy, and the crystal quality of the subsequent *p*-GaN layer will be degraded. Most importantly, the hole injection cannot be improved effectively due to the existence of the ΔE_v between the last GaN barrier and the EBL.⁵ In this paper, we designed a graded-composition EBL (GEBL) for InGaN/GaN LEDs employing the concept of band-engineering, which not only suppressed the electron overflow out of active region but also enhanced the hole injection. The improvements in electron confinement and hole injection of LED with GEBL were demonstrated in simulation. Then it was realized by using metal-organic chemical vapor deposition (MOCVD), and the efficiency droop in LED with GEBL was found to be much smaller

than that in conventional LED with constant-composition Al_xGa_{1-x}N EBL.

The concept of band-engineering started from the observation on the band diagram of InGaN/GaN LEDs. For conventional LEDs operated under forward bias, the band diagram of EBL shows a triangular shape due to the internal polarization field and forward bias,⁸ as shown in Fig. 1. The valence band of EBL slopes upward from the *n*-GaN side toward the *p*-GaN side, which retards the holes to transport across the triangular barrier. But if the composition of aluminum in EBL increases from the *n*-GaN side toward the *p*-GaN side, the band-gap broadens gradually. As a result, the barrier in the valence band could be level down and even overturn, while the slope of the conduction band could be enhanced. Then, the improvement in capability of hole transportation across the EBL as well as the electron confinement could be expected.

To prove the feasibility of the hypothesis above, the band diagrams and carrier distributions in LED with GEBL

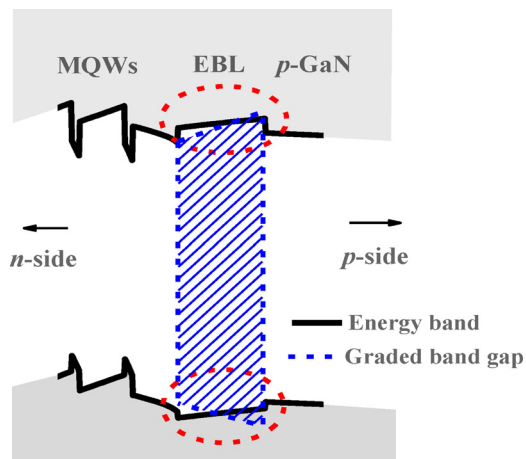


FIG. 1. (Color online) Schematic diagram of the concept of band-engineering at EBL.

^{a)}Electronic mail: josephwang.eo97g@nctu.edu.tw.

^{b)}Electronic mail: jchli@mail.nctu.edu.tw.

^{c)}Electronic mail: hckuo@faculty.nctu.edu.tw.

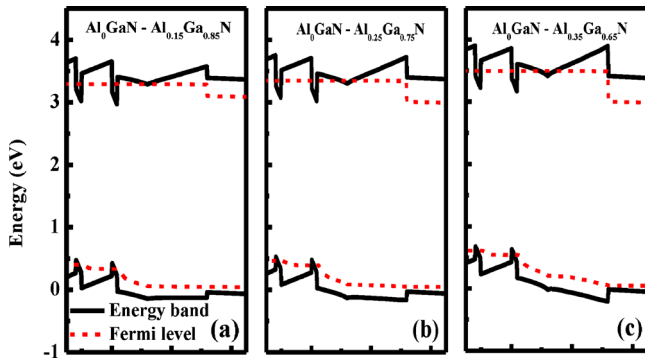


FIG. 2. (Color online) Calculated energy band diagrams of (a) Al_0GaN to $\text{Al}_{0.15}\text{Ga}_{0.85}\text{N}$, (b) Al_0GaN to $\text{Al}_{0.25}\text{Ga}_{0.75}\text{N}$, and (c) Al_0GaN to $\text{Al}_{0.35}\text{Ga}_{0.65}\text{N}$ graded-composition EBLs at a current density of 100 A/cm^2 .

were investigated first by APSYS simulation program. The simulation LED structures were composed of $4\text{-}\mu\text{m}$ -thick n -type GaN layer (n -doping = $2 \times 10^{18} \text{ cm}^{-3}$), six pairs of $\text{In}_{0.15}\text{Ga}_{0.85}\text{N}/\text{GaN}$ multiple-quantum wells (MQWs) with 2.5-nm -thick wells and 10-nm -thick barriers, 20-nm -thick $p\text{-Al}_x\text{Ga}_{1-x}\text{N}$ EBL or GEBL (p -doping = $5 \times 10^{17} \text{ cm}^{-3}$), and 200-nm -thick p -type GaN layer (p -doping = $1 \times 10^{18} \text{ cm}^{-3}$). For the LEDs with GEBL, three types of GEBLs with compositions of aluminum graded along the $[0001]$ direction from 0% to 15% , 25% , and 35% , respectively, were simulated and denoted as LEDs A, B, and C. Furthermore for the conventional LED, the composition of aluminum was a constant of 15% . Commonly accepted physical parameters were adopted to perform the simulations, the percentage of screening effect of 50% , the Shockley–Read–Hall recombination lifetime of 1 ns , and the Auger recombination coefficient in quantum wells of $2 \times 10^{-30} \text{ cm}^6/\text{s}$, respectively.⁹ Other material parameters used in the simulation can be referred to Ref. 10.

Figure 2 shows the energy band diagrams of LEDs A, B, and C at current density of 100 A/cm^2 . According to our concept of band-engineering, the degree of gradation had the decisive influence on the capability of hole injection. Even with small degree of gradation as LED A, the slope of the valence band can be leveled. Then the slope starts to overturn when the composition of aluminum at the p -side increases up to 25% . Moreover, it is worth noting that the ΔE_v between the last GaN barrier and the EBL is diminished in all three LEDs with GEBL. Therefore, the hole injection can be improved effectively by using the GEBL. In the meantime, as the degree of gradation increased, the conduction band offset at the interface of p -GaN and EBL increases as well, so does the confinement capability of electrons. But correspondingly, the ΔE_v between EBL and p -GaN increases

as the composition of aluminum rises, which might retard the transportation of holes. In addition, high aluminum-composition EBL is not practical for actual application due to the low acceptor-activation efficiency and the low crystal quality in epitaxy.¹¹ Consequently, only LED B with aluminum graded from 0% to 25% is discussed in the following paragraph.

The profiles of hole and electron concentration distribution at a current density of 100 A/cm^2 are illustrated in Figs. 3(a) and 3(b), respectively. It can clearly be seen that with GEBL, injected holes uniformly distribute along the EBL region compared to conventional one, demonstrating that the flat valence band indeed favored the hole transportation across EBL. Meanwhile, the hole concentration in MQWs is significantly increased as expected. Moreover, the electron concentration in MQWs is also enhanced, while the electron distribution within the GEBL region and p -GaN is enormously decreased over two orders. This result indicates that GEBL can suppress the electron overflow out of active region more effectively than conventional EBL, even though the conduction band offset between the last GaN barrier and the GEBL is diminished.

Then, the LED structures with EBL and GEBL were grown on c -plane sapphire substrates by MOCVD. After depositing a low temperature GaN nucleation layer, a $4 \mu\text{m}$ n -type GaN layer, and a ten-pair InGaN/GaN superlattice prestrain layer, the rest of the LED structures were grown based on our simulation design. The epitaxial recipe for the GEBL is worth noting. Generally, the graded-composition ternary III-nitride semiconductors can be grown by two methods: growth temperature ramping and III/III ratio ramping.^{12,13} Here we adopted the Al/Ga ratio ramping because the temperature ramping would change the growth rate, and the higher temperature might damage the quality of QWs. The growth temperature of conventional EBL and GEBL was the same ($870 \text{ }^\circ\text{C}$), and the aluminum-composition profile of the GEBL was approximately graded from 0% to 25% . Finally, the LED chips were fabricated by regular chip process with ITO current spreading layer and Ni/Au contact metal, and the size of mesa is $300 \times 300 \mu\text{m}^2$. The emission wavelengths of both LEDs were around 450 nm at 22 A/cm^2 .

Figure 4 shows the L - I - V curves of the conventional and GEBL LEDs. The output powers were measured with a calibrated integrating sphere. The forward voltages (V_f) at 22 A/cm^2 and series resistances (R_s) of GEBL LED are 3.28 V and 7Ω , respectively, which are lower than that of 3.4 V and 8Ω for conventional LED. The reduced V_f and R_s can be attributed to the improvement in hole injection and the higher-efficiency p -type doping in GEBL.¹⁴ In the case of

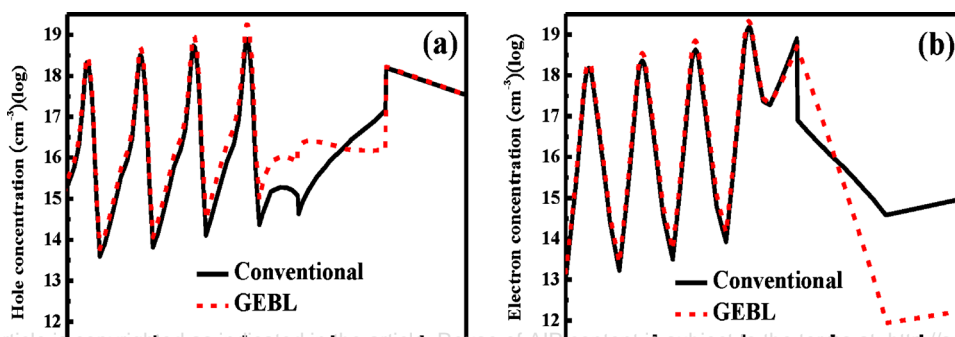


FIG. 3. (Color online) Calculated (a) hole concentration distribution and (b) electron concentration distribution of conventional and GEBL LEDs at a current density of 100 A/cm^2 .

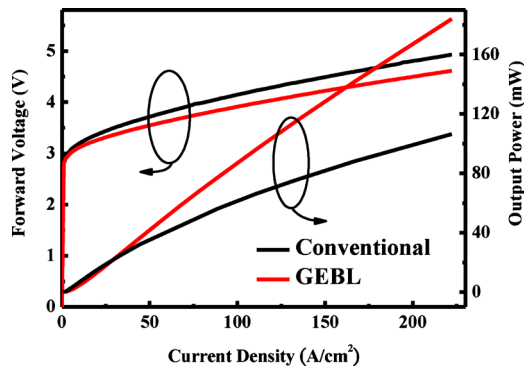


FIG. 4. (Color online) Forward voltage and output power as a function of current density for conventional and GEBL LEDs.

L - I curves in Fig. 4, although the output power of GEBL LED is a little lower at low current density (below 30 A/cm^2), it increases more rapidly as the injection current increases as compared to the conventional one. The output powers were enhanced by 40% and 69% at 100 and 200 A/cm^2 , respectively. This phenomenon can be explained as follows: at low current density, it is more difficult for holes to tunnel across the barrier at the interface of p -GaN and EBL in GEBL LED because the ΔE_v is larger than that in conventional LED. While at high current density, the tunneling process of holes can be negligible, and the diffusion process is dominated for the hole transportation into the MQW.⁵ As discussed above, the diffusion process in GEBL is much easier than that in conventional one due to the flat valence band and much lower ΔE_v at the interface of the last GaN barrier and EBL. In conjunction with the superior electron confinement, much stronger light output was achieved in GEBL LED at high current density.

Finally, the normalized efficiency of conventional and GEBL LEDs as a function of current density was investigated, as shown in Fig. 5. The maximum efficiency (η_{peak}) of GEBL LED appears at an injection current density of 80 A/cm^2 , which was much higher than that for conven-

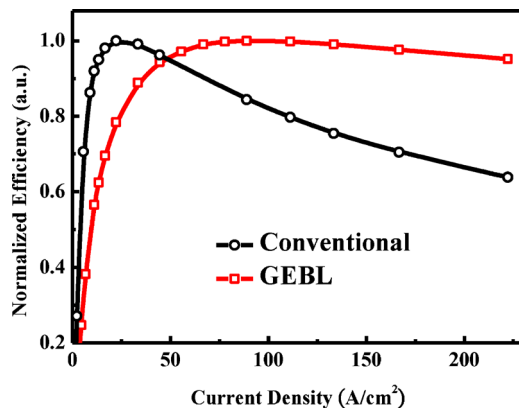


FIG. 5. (Color online) Normalized efficiency as a function of current density for conventional and GEBL LEDs.

tional LED (at 20 A/cm^2). More interestingly, the efficiency droop, defined as $(\eta_{\text{peak}} - \eta_{200 \text{ A/cm}^2}) / \eta_{\text{peak}}$, was reduced from 34% in conventional LED to only 4% in GEBL LED. This significant improvement in efficiency can be mainly attributed to the enhancement of hole injection as well as electron confinement, especially at high current density.

In conclusion, we have designed a graded-composition electron blocking layer for InGaN/GaN LED by employing the band-engineering. The simulation results showed that the triangular barrier of conventional EBL at the valence band could be balanced, while the slope of the conduction band could be increased by increasing the band-gap of $\text{Al}_x\text{Ga}_{1-x}\text{N}$ along the $[0001]$ direction. As a result, the hole concentration in MQWs was significantly increased, while the electron distribution within the GEBL region and p -GaN was enormously decreased over two orders, indicating that the GEBL can effectively improve the capability of hole transportation across the EBL as well as the electron confinement. Furthermore, the LED structure with GEBL was realized by MOCVD. The L - I - V characteristics of GEBL LED showed the smaller V_f and R_s due to the improvement in hole injection and the higher-efficiency p -type doping in GEBL as compared to the conventional LED. More importantly, the efficiency droop was reduced from 34% in conventional LED to only 4% in GEBL LED. This work implies that carrier transportation behavior could be appropriately modified by employing the concept of band-engineering.

The authors would like to thank Dr. T. C. Hsu and Dr. M. H. Shieh of Epistar Corporation for their technical support. This work was funded by the National Science Council of Taiwan under Grant No. NSC 98-3114-M-009-001 and NSC 98-3114-E-009-002-CC2.

¹U.S. Department of Energy, <http://www.energy.gov/>.

²M.-H. Kim, M. F. Schubert, Q. Dai, J. K. Kim, E. Fred Schubert, J. Piprek, and Y. Park, *Appl. Phys. Lett.* **91**, 183507 (2007).

³C. H. Wang, J. R. Chen, C. H. Chiu, H. C. Kuo, Y. L. Li, T. C. Lu, and S. C. Wang, *IEEE Photonics Technol. Lett.* **22**, 236 (2010).

⁴A. David, M. J. Grundmann, J. F. Kaeding, N. F. Gardner, T. G. Mihopoulos, and M. R. Krames, *Appl. Phys. Lett.* **92**, 053502 (2008).

⁵S.-H. Han, D.-Y. Lee, S.-J. Lee, C.-Y. Cho, M.-K. Kwon, S. P. Lee, D. Y. Noh, D.-J. Kim, Y. C. Kim, and S.-J. Park, *Appl. Phys. Lett.* **94**, 231123 (2009).

⁶S. Choi, H. J. Kim, S.-S. Kim, J. Liu, J. Kim, J.-H. Ryou, R. D. Dupuis, A. M. Fischer, and F. A. Ponce, *Appl. Phys. Lett.* **96**, 221105 (2010).

⁷Y. K. Kuo, M. C. Tsai, and S. H. Yen, *Opt. Commun.* **282**, 4252 (2009).

⁸S. C. Ling, T. C. Lu, S. P. Chang, J. R. Chen, H. C. Kuo, and S. C. Wang, *Appl. Phys. Lett.* **96**, 231101 (2010).

⁹J. Piprek, *Nitride Semiconductor Devices: Principles and Simulation* (Wiley-VCH, Berlin, 2007), p. 279.

¹⁰I. Vurgaftman and J. R. Meyer, *J. Appl. Phys.* **94**, 3675 (2003).

¹¹M. Katsuragawa, S. Sota, M. Komori, C. Anbe, T. Takeuchi, H. Sakai, H. Amano, and I. Akasaki, *J. Cryst. Growth* **189–190**, 528 (1991).

¹²C. K. Sun, T. L. Chiu, S. Keller, G. Wang, M. S. Minsky, S. P. DenBaars, and J. E. Bowers, *Appl. Phys. Lett.* **71**, 425 (1997).

¹³M.-H. Kim, Y.-G. Do, H. C. Kang, D. Y. Noh, and S.-J. Park, *Appl. Phys. Lett.* **79**, 2713 (2001).

¹⁴J. Simon, V. Protasenko, C. Lian, H. Xing, and D. Jena, *Science* **327**, 60 (2010).